Hybrid Integration of a Bowtie Slot Antenna and a Quantum Dot Mode-Locked Laser

Junghoon Kim, Christos G. Christodoulou, Z. Ku, Chang-Yi Lin, Yongchun Xin, Nader A. Naderi, and Luke F. Lester

Abstract—This letter discusses the integration of a mode-locked quantum dot (QD) laser and an antenna. A brief theory of operation for the reconfigurable mode-locked QD laser is first presented, and the design of the antenna as well as the matching network used to connect the photonic source to the antenna are explained and discussed. The ultimate goal is to achieve a compact RF/photonic chip that can radiate from 10 to 100 GHz. Here, we present the initial proof of concept and the challenges associated with integrating the antenna with the QD mode-locked laser.

Index Terms—Bowtie antenna, mode-locked laser, quantum dot (QD).

Fig. 1. Quantum dot mode-locked laser.

I. INTRODUCTION

ONE of the primary interests of modern microwave and communication technologies is to produce compact and reconfigurable sources on a chip that can be used for various frequencies and applications. Here, we present a new, integrative approach to achieve such a device by marrying microwave and optical techniques. A new approach to generate RF pulse signals is presented. We start with an array of quantum dot (QD) diode cells configured to emit mode-locked laser pulses. By manipulating the biasing of the saturable absorber (SA) section of a QD mode-locked laser (QD-MLL), we can control the various resonance frequencies generated. These microwave signals are then transported by a coplanar waveguide (CPW) to a bowtie slot antenna. The bowtie slot antenna, lithographically printed on the dielectric surface, has been selected as the appropriate type of antenna to couple to the active optoelectronic RF source due to its simple design and broadband impedance characteristics. Moreover, its fabrication is well suited to RF-photonic integrated circuit technology [1], [2]. This letter describes the principles of the QD-MLL, the antenna design, and their matching circuit. Both our preliminary simulated and measured results are presented and discussed to support our proof of concept.

J. H. Kim and C. G. Christodoulou are with Department of Electrical and Computer Engineering, University of New Mexico, Albuquerque, NM 87131 USA (e-mail: jkim13@ece.unm.edu; christos@ece.unm.edu).

Z. Ku, C.-Y. Lin, N. A. Naderi, and L. F. Lester are with Center for High Technology Materials, University of New Mexico, Albuquerque, NM 87131 USA (e-mail: cylin@unm.edu; nader@chtm.unm.edu; luke@chtm.unm.edu).

Y.-C. Xin is with IBM Systems and Technology Group, Semiconductor Solutions, Hopewell Junction, NY 12533 USA (e-mail: ycxin@chtm.unm.edu).

Color versions of one or more of the figures in this letter are available online at http://ieeexplore.ieee.org.

Digital Object Identifier 10.1109/LAWP.2009.2038345
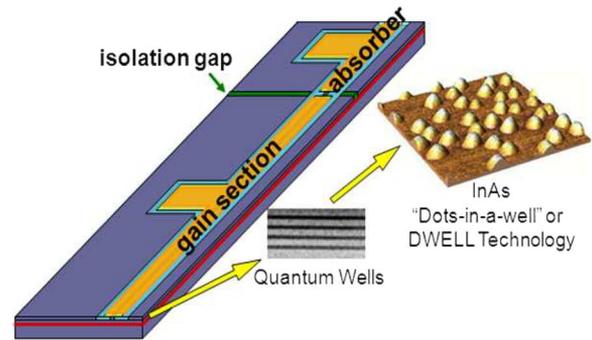
II. THE QUANTUM DOT MODE-LOCKED LASER

The subject of stable, optoelectronic RF sources has received considerable interest recently as higher operating frequencies are demanded [3], [4] since solid-state electronics has inevitable limitations in high-frequency applications mainly due to high dielectric losses. In our work, we start with an optical pulse generation technique using a mode-locked laser. A two-section QD passively mode-locked laser is shown in Fig. 1. As a picosecond optical pulse goes into the SA, the leading edge of the optical pulse is absorbed and creates free carriers. The resulting electrons and holes are swept to the metal contacts as the photocurrent due to the built-in electrical field. Thus, a RF signal can be generated and controlled by using only a dc bias. There are several prime advantages in using the QD-MLL as a source. It has an expanded range of stable mode-locking operation so that it permits higher RF power to be extracted from the device. This method is able to obtain higher optical-to-electrical conversion efficiency compared to competing approaches such as an optical heterodyning technique of two lasers [5]. Another merit of this approach is the easier stabilization of the generated frequency by removing the uncorrelated phase noise [6]. The QD-MLL, depicted in Fig. 1, uses a multistack "dots-in-a-WELL" (DWELL) active region that embeds InAs dots within an InGaAs quantum well sandwich layer [7], [8]. The saturable absorber of the QD-MLL is electrically similar to a reverse-biased, high-speed photodiode. Using its absorber section, a passive QD-MLL can stably provide a microwave signal without the additional optical-to-electrical conversion process such as in low-temperature photoconductors. Therefore, with respect to RF systems, it is possible to achieve a compact system on a chip by implementing the QD-MLL as an input. By adjusting the round-trip time in the QD-MLL, one can alter the frequency

TABLE I
IMPEDANCE AND S11 IN dB IMPROVEMENT BY MATCHING CIRCUIT

Cases	Frequency [GHz]	Impedance [Ω]	S11 [dB]
Unmatched	10	4.45-j8.25	-1.5
	20	6.95-j8.2	-2.37
Matched	10	74.75-j1.3	-14
	20	39.25-j13.05	-14.5

Fig. 2.   Bowtie slot antenna with a short stub matching.

Fig. 3.   Return loss in decibals of a bowtie slot antenna.
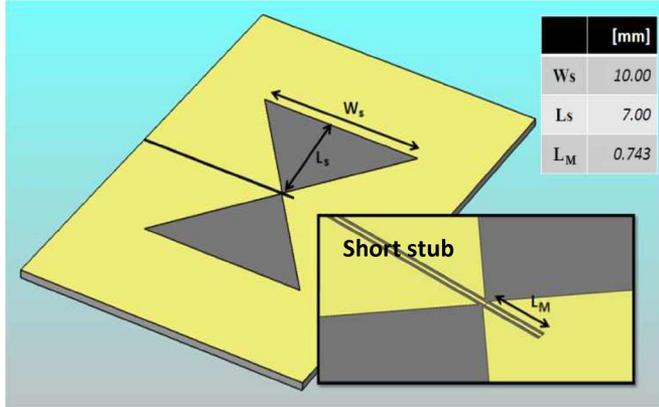
at which a microwave signal gets generated. The frequency of generated pulses in a QD-MLL can be predicted with [9]

$$f = \frac{c}{2n_{\text{eff}}L} \tag{1}$$

where c is the speed of light in vacuum, n_{eff} is the group effective refractive index of the quantum dot waveguide, and L is the cavity length of laser. This is a very important feature, especially when the antenna connected to this new source is also reconfigurable or wideband. In our case, for a 4.1-mm-long QD-MLL, the frequency of the first harmonic is computed as approximately 10 GHz. In the next section, we discuss the details of the antenna selected to match this new photoelectronic source.

III. ANTENNA AND MATCHING CIRCUIT

A. Antenna Configuration

Among the possible candidates, a bowtie slot antenna is chosen to incorporate with the QD-MLL. The desired operating frequencies of the proposed bowtie slot antenna are the first and second harmonics of the QD-MLL. As illustrated in Fig. 2, a semi-insulating GaAs material with permittivity of 12.9 and 450 μm thickness is selected as the antenna substrate. The same material used for the laser chip is also used as the substrate for the antenna for the monolithic fabrication of the entire RF/photonic device. A CPW is used to feed the bowtie antenna. To realize a 50-Ω characteristic impedance with this CPW, the width is determined as 54.14 μm and that of the air gap as 40 μm. The optimized width of the triangle bow ($\mathbf{W_s}$) for the antenna is 10 mm, and the length of the triangle ($\mathbf{L_s}$) is chosen as 7 mm.
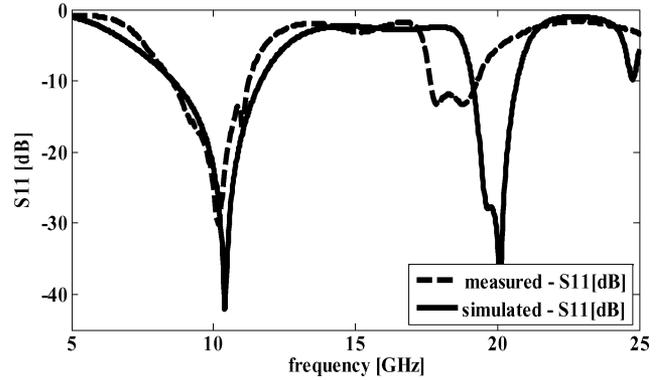
A short stub with length $\mathbf{L_M}$ is used to match the antenna to the 50 Ω at the desired frequencies. Fig. 3 shows the comparison between the measured and simulated S11 results of the bowtie slot antenna. These results are only for the antenna matched to the CPW and do not include the matching of the QD-MLL device yet. One can see that the matching is much better at 10 GHz than at 20 GHz, which indicates that either a much broader matching network should be used or one can try to fix that problem when the QD-MLL is connected. Two reactive matching stubs in series are used to resolve its mismatching problem. The details of matching of the QD-MLL to the antenna are discussed next.

B. Matching Circuit

Here, we start with the S11 measurement of the QD absorber over the frequency range from 0 to 30 GHz. Based on the measured S11 data, one can recalculate the output impedances of the absorber at both the first and second harmonic frequencies (10 and 20 GHz). As indicated in Table I, the output impedances of the absorber section are about 4-j8 Ω at 10 GHz and 6-j8 Ω at 20 GHz, respectively. Fig. 4 shows the equivalent circuit model of the impedance transformer used, which consists of two open stubs combined in parallel. The actual matching structure is shown in Fig. 5, and its dimensions are provided in Table II. By using both microwave circuit design (ADS) and full-wave analysis tools (CST), one can optimize the matching circuit to the desired 50 Ω. Without the aid of impedance matching, the amounts of delivered power are only 29% (at 10 GHz) and 43% (at 20 GHz) of the generated power. After applying the matching circuit, the gain is calculated as 5.3 dB at 10 GHz and 3.7 dB at 20 GHz according to the transmitted power ratio; $20log_{10}(\mathbf{T}_{\text{matched}}/\mathbf{T}_{\text{unmatched}})$, where $\mathbf{T} = \mathbf{S(2,1)}$ [10]. Both the calculated gain and numerical S11 comparison in dB value for the matched and unmatched cases are presented in Fig. 6.

TABLE II
DIMENSIONS OF A MATCHING CIRCUIT

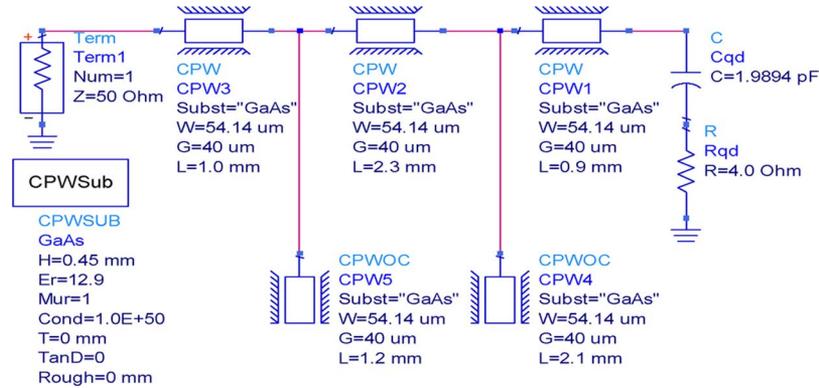| CPW (A)		Stub1 (B)	Stub2 (C)			Unit: mm
W	G	L_p2	L_p1	L_s1	L_s2	L_s3
0.054	0.04	1.22.1	2.11.2	0.9	2.3	1.0

Fig. 4.   Equivalent circuit model of the matching network.
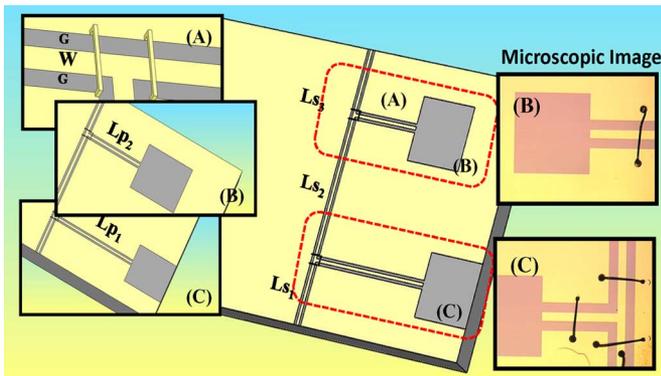

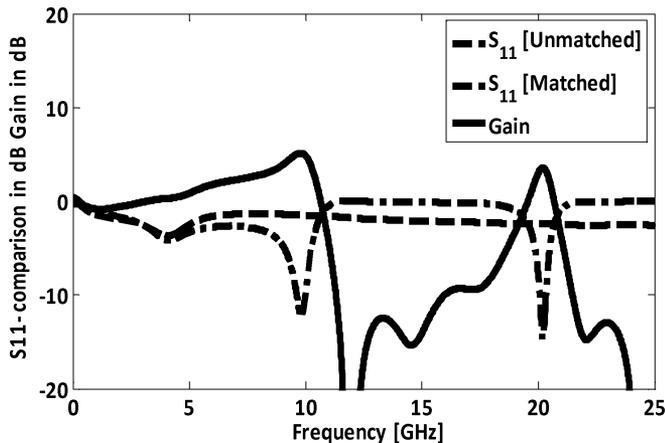Fig. 5.   Schematic view of an impedance transformer and microscopic images of open stubs.

Fig. 6.   Gain and S11 comparison in decibals for with/without a matching circuit.

C. Fabrication Flow of the Antenna With Matching Circuit

At first, a layer of negative AZ 5214E-IR photoresist (PR) is applied to the 450-μm-thick SI-GaAs substrate. Using a photolithographic technique, a coherent UV laser beam (third harmonic of a YAG laser at $\lambda = 0.405$ nm) is applied to make the antenna image appear in the PR layer. Next, an e-beam metal evaporation is used to deposit thin films of Ti (0.05 μm) and Au (0.3 μm) atop the PR layer. The Ti material was used to improve adhesion between a GaAs layer and a thin Au film. The final structure is followed by a liftoff process using acetone to remove the PR.

IV. MEASUREMENTS

The photocurrent from the QD-MLL was measured under the bias conditions of both the 1-V reverse dc voltage and the 200 mA forward current. In Fig. 7, the measured spectrum of the photocurrent shows that the fundamental harmonic frequency is 10.2 GHz. The result agrees well with a calculated frequency according to the (1). The measured intensity at 10.2 GHz is around -3 dBm (501 μW), and that of the second harmonic (20 GHz) is decreased to -17 dBm (19.95 μW).

The experiment to measure the received power from the QD-MLL-excited antenna was performed next. The schematic for the experimental setup is illustrated in Fig. 8, where it is composed of a spectrum analyzer (*Agilent* 8565EC), a bias-tee (*HP* 33150A), and an X-band horn antenna. The approximate straight-line distance between the transmitter and the receiver antennas is 10 cm. According to the measured spectrum shown in Fig. 9, the measured intensity of the radiation is -52 dBm (10 nW) at 10 GHz.
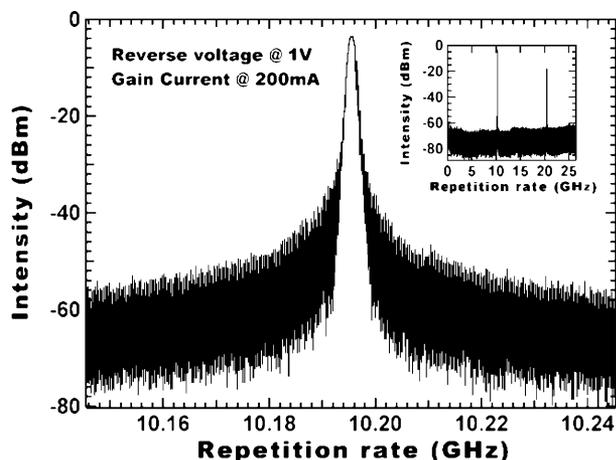
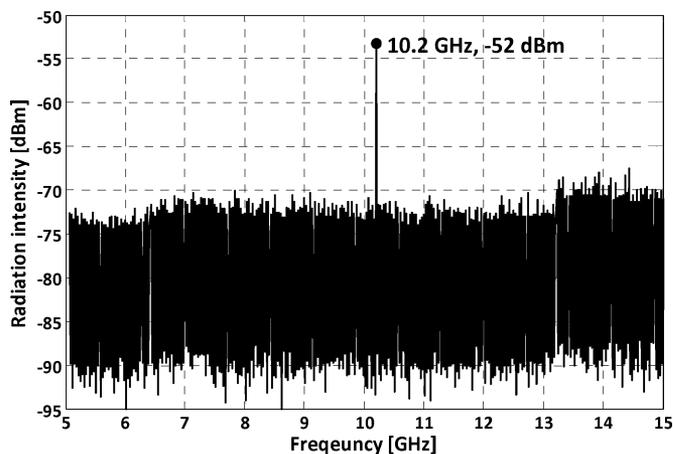Fig. 7. Electrical spectrum analyzer (ESA) spectrum of photocurrent.

Fig. 8. Radiation intensity experimental setup.
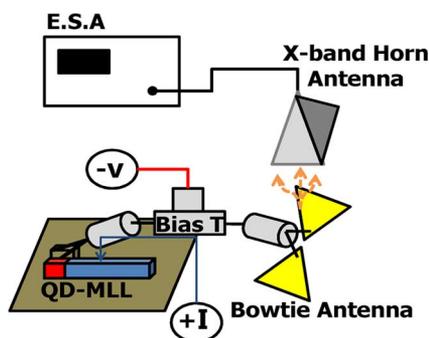

Fig. 9. ESA spectrum of a radiation from an antenna.

V. CONCLUSION

In our preliminary work, we have shown that we can directly connect a QD-MLL device to an antenna and radiate power. The photocurrent intensity of the QD-MLL can be improved by optimizing the biasing conditions. To improve the radiation efficiency at the first and second harmonics, a matching circuit was designed and applied to the antenna. Under matched conditions, the transmitted power to the antenna is improved by 5 dB at 10 GHz and 3.7 dB at 20 GHz. Future work will focus on increasing the conversion efficiency of the laser and the seamless integration of the antenna with the laser source and reducing the phase noise of the generated RF signal.

REFERENCES

[1] C. R. Brewitt-Taylor, D. J. Gunton, and H. D. Rees, "Planar antennas on a dielectric surface," *Electron. Lett.*, vol. 12, pp. 729–731, 1981.

[2] J. H. Kim, C. G. Christodoulou, Z. Ku, Y.-C. Xin, N. A. Naderi, and L. F. Lester, "Quantum-dot laser coupled bowtie antenna," in *Proc. IEEE AP-S* , Jul. 5–11, 2008, pp. 1–4.

[3] G. A. Vawter, A. Mar, V. Hietala, J. Zolper, and J. Hohimer, "All optical millimeter-wave electrical signal generation using an integrated mode-locked semiconductor ring laser and photodiode," *IEEE Photon. Technol. Lett.*, vol. 9, no. 12, pp. 1634–1636, Dec. 1997.

[4] M. Passerini, M. Sorel, and P. J. R. Laybourn, "Optimisation and regime characterization of monolithic semiconductor mode-locked lasers and colliding-pulse mode-locked lasers at microwave and millimeter-wave frequencies," *IEE Proc. Optoelectron.*, vol. 151, no. 6, pp. 508–512, Dec. 2004.

[5] J. Genest, M. Chamberland, P. Tremblay, and M. Tetu, "Microwave signals generated by optical heterodyne between injection-locked semiconductor lasers," *IEEE J. Quantum Electron.*, vol. 33, no. 6, pp. 989–998, Jun. 1997.

[6] A. Gubenko, D. Livshits, I. Krestnikov, S. Mikhrin, A. Kozhukhov, A. Kovsh, N. Ledentsov, A. Zhukov, and E. Portnoi, "High-power monolithic passively mode-locked quantum-dot laser," *Electron. Lett.*, vol. 41, no. 20, pp. 1124–1125, Sep. 29, 2005.

[7] E. U. Rafailov, M. A. Cataluna, and W. Sibbett, "Mode-locked quantum-dot lasers," *Nature Photon.*, vol. 1, pp. 395–401, Jul. 2007.

[8] Y. C. Xin, Y. Li, V. Kovanis, A. L. Gray, L. Zhang, and L. F. Lester, "Reconfigurable quantum dot monolithic multi-section passive mode-locked lasers," *Opt. Exp.*, vol. 15, no. 12, pp. 7623–7633, 2007.

[9] J. T. Verdeyen, *Laser Electronics*, ser. Solid State Physical Electronics, 3rd ed.   Englewood Cliffs, NJ: Prentice-Hall, 1995, ch. 9, p. 297.

[10] J. H. Kim, C. G. Christodoulou, Z. Ku, C.-Y. Lin, N. A. Naderi, L. F. Lester, and J. P. Kim, "A bowtie slot antenna coupled to a quantum-dot mode locked laser," in *Proc. IEEE APSURSI*, Jun. 1–5, 2009, pp. 1–4.